

## Physical Vapor Deposition of Nanocrystalline Composites of Ag-Ni for Electrical Contacts in Automotive Industries

Shehdeh Jodeh\*

Department of Chemistry, Najah University, Nablus, Palestine. E-mail: [sjodeh@hotmail.com](mailto:sjodeh@hotmail.com);  
Tel: 972-92995744; Fax: 972-92347488.

Received on June 28, 2008

Accepted on Sept. 22, 2008

### Abstract

Using vapor deposition as a tool, novel coating structures have been developed for low friction coefficient, fretting wear resistant and high temperature stable electrical contacts. Thin films of Ag-Ni nanocrystalline composites between 100 and 500-nm thick were deposited by electron beam evaporation onto sputter-cleaned 301 stainless steel substrates. The structure and composition of the films were studied in detail using x-ray diffraction (XRD), scanning electron microscopy (SEM), electron probe microanalysis (EPMA), and Auger depth profiling. The contact properties, such as contact resistance, friction coefficient, fretting wear resistance, and thermal stability of these coatings have been measured. Both the Ag and Ag<sub>81</sub>Ni<sub>19</sub> composite coatings about 500-nm thick passed the 1,000,000 cycle fretting wear test. These coatings also showed good high temperature stability during heat-aging at 150 °C in air, especially the Ag<sub>81</sub>Ni<sub>19</sub> composite coating. This study shows that vapor deposition is a powerful technique which can be used to discover new coating compositions and structures for electrical contact applications.

**Keywords:** Coating; Adhesion; Wear; Vacuum; Friction.

### Introduction

Automotive vehicles have an increasing content of electrical and electronics component which requires wires with electrical terminals. Those electrical materials consist of soft, high conductivity, oxidation resistance materials<sup>[1-3]</sup>. This increased in the number of electrical contacts accompanied with increased in the number of attached around the engines in the underhood compartment will reduce ambient cooling of the compartment area and increase the temperature of the engine<sup>[4-5]</sup>. Operation of the engines causes vibrations, underhood electrical connections on automotive can be exposed to temperatures reached over 150 °C. The vibration resistance of a connector can be improved by minimizing the relative movement at contact interfaces. This normally requires improved connector locks, seals, and harness strain relief features, which add to the cost of the vehicle. This normally requires electrical contact and electrode materials consist of soft-high conductivity, oxidation resistant materials. Electroplated silver has been widely identified as a high

---

\* Corresponding author. e-mail: [sjodeh@hotmail.com](mailto:sjodeh@hotmail.com)

temperature coating materials for electrical connector applications. Silver coatings are not highly resistant to corrosion and generally characterized by a high coefficient of friction, on the order of about one for silver on silver<sup>[6-7]</sup>.

Due to the general increase in the number and complexity of electronic components and systems used in the automotive, computer, and telecommunications fields, a need exists for increasing the number of circuits per connector without significantly increasing the mating force required to join these additional circuits<sup>[8, 9]</sup>. Additionally, this increase in the number of components leads to a need for reducing connector size, and therefore terminal cross-section area. However, a reduction in connector size can lead to an increase in the occurrence of damages to connectors, such as from terminal bending or breakage, upon connector insertion.<sup>[10]</sup> The demand for reliable, economical, and environmentally benign electrical connectors is expected to grow. To ensure reliable electrical contacts, various coatings are applied to the connectors. Presently, most connectors used in automobiles are electroplated with tin (Sn)<sup>[11]</sup>.

In this study, we use vapor deposition as a tool to investigate coating structures and compositions that meet the requirements of low friction coefficient and high temperature stability as well as excellent fretting wear resistance. Previous studies on vapor deposited thin silver and nickel have demonstrated good performance for low friction and high temperature electrical contact applications<sup>[12]</sup>. To have a complete understanding of a vapor deposition in improving electrical contacts thin coatings of Ag-Ni composites are deposited on 301 steel by electron beam evaporation in ultrahigh vacuum. Fretting wear, friction coefficients, and thermal stability of these coatings are studied. Promising compositions and structures for low friction coefficient, fretting wear resistant, and high temperature stable coatings are identified.

## **Experimental**

Thin films of Ag-Ni were prepared by electron beam evaporation in ultrahigh vacuum. The evaporation source materials are 99.999% pure Ag (Johnson-Matthey) and 99.99% pure Ni (Johnson-Matthey) located in two separate electron-beam evaporation sources. The substrates were 301 stainless steel plates, hemispherical 301 stainless steel dimples of 1.6-mm radius, and oxidized silicon wafers. They were cleaned in an ultrasonic bath first with acetone, then with methanol for at least 15 min each before loading into the loadlock of the deposition chamber. The substrates were introduced into the deposition chamber when the pressure in the loadlock was less than  $2 \times 10^{-7}$  Torr. The base pressure of the deposition chamber was typically in the mid  $10^{-9}$  Torr range and always lower than  $1 \times 10^{-8}$  Torr. Before deposition the surface of the substrates was sputter cleaned using 100 eV Ar<sup>+</sup> with a beam current density of about  $1 \text{ mA/cm}^2$  for 5 minutes. Previous experiments have shown

improved adhesion between films and substrates by sputter cleaning <sup>[13]</sup>. The Ag-Ni composite coatings were obtained by evaporating Ag and Ni simultaneously from two electron beam evaporation sources. The substrate temperature initially was at room temperature (25 °C) and increased to 51°C or less during all depositions. The deposition rate of each material, typically a few tenths of a nm per second, was controlled by an Inficon IC4 Plus quartz crystal monitor. During the deposition of Ag-Ni composites, the rates were specified such that the desired composition in the film was achieved. The low pressure during deposition ensures the high purity of the films. The total impurity level of oxygen and carbon typically less than 2 at.% measured by Auger electron spectroscopy (AES). The deposition system has been used to examine thin film growth, structure, and properties, including epitaxial metallic layers, nanocrystalline composites, amorphous materials, and their mechanical and electrochemical properties <sup>[14]</sup>.

The structure composition analysis and fretting wear test including contact resistance measurements were discussed in details in previous study<sup>[15]</sup>.

## **Results and Discussion**

### *Structure and Composition*

X-ray diffraction results of the Ag<sub>49</sub>Ni<sub>51</sub> and Ag<sub>81</sub>Ni<sub>19</sub> films are shown in Fig. 1 together with that of a pure Ag and a pure Ni film. The overall composition and thickness were determined by EPMA. The two broad diffraction peaks in the diffraction pattern from Ag<sub>49</sub>Ni<sub>51</sub>, one at a slightly higher angle than that of Ag(111) and the other at a slightly lower angle than that of Ni(111) peak, suggest that the film consists of a Ag-rich phase and a Ni-rich phase rather than a single, face-centered-cubic (fcc) solid solution. If there were a single fcc solid solution, the two peaks would have been at higher angles than the respective Ag(111) and Ag(200) peaks. These peak shifts are the result of lattice parameter differences between Ag (4.0862 Å) and Ni (3.5238 Å) <sup>[16]</sup>. Similarly, the Ag<sub>81</sub>Ni<sub>19</sub> film is a composite consisting of a Ag-rich and a Ni-rich phase, although the second diffraction peak was small and could only be observed in the log (intensity) vs. angle plot (data not shown).

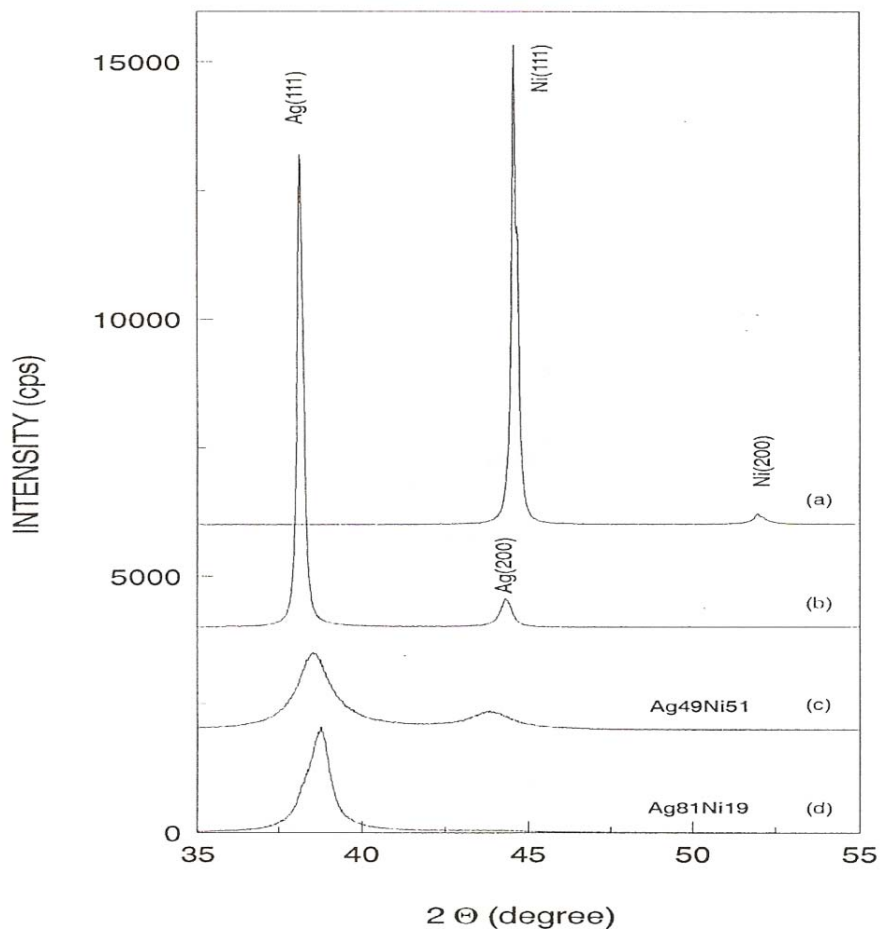


**Figure 1.** The  $\theta$ - $2\theta$  XRD patterns of a Ni thin film (a), Ag thin film (b) Ag<sub>49</sub>Ni<sub>51</sub> thin film (c), and Ag<sub>81</sub>Ni<sub>19</sub> thin film (d)

The average grain size can be determined, using the Scherrer formula, from the full width at half maximum (FWHM) of the diffraction peaks. The concentration of each phase can be determined from peak positions using Vegard's law <sup>[17]</sup> which states that lattice parameter is linearly proportional to atomic concentration. The results of these analysis are given in Table 1. Thus, nanocrystalline composites of a Ag-rich and a Ni-rich phase have been made by co-deposition of Ag and Ni at room temperature onto both oxidized silicon and 301 steel substrates.

**Table 1.** Grain size and composition of the Ag-Ni composite thin films made by electron beam evaporation.

Samples	Ag-rich phase (at.% Ag)	Ni-rich phase (at.% Ni)	Grain Size (nm)	
			Ag-rich phase	Ni-rich phase
Ag <sub>49</sub> Ni <sub>51</sub>	92	90	9	9
Ag <sub>81</sub> Ni <sub>19</sub>	89	*	13	*

\* Diffraction peak is too weak for accurate determination.

The formation of nanocrystalline composites of Ag and Ni can be understood from the following thermodynamic and kinetic considerations. Because of the positive heat of mixing, Ag and Ni are mutually insoluble in thermodynamic equilibrium <sup>[18, 19]</sup>. When Ag and Ni atoms are deposited onto substrates simultaneously, phase separation is expected.

However, because atomic diffusion is limited at low substrate temperature (e.g., 25°C), the size of the phase-separated region is small and some degree of solute trapping can produce supersaturated solid solution as observed in Fig. 1 and Table 1. Similar observations have been made in co-deposited Al and Ge and co-deposited Ag and Mo <sup>[20, 21]</sup>. The latter has been suggested as a coating for reducing friction and wear <sup>[21]</sup>.

#### *Fretting Wear*

The fretting wear results of the 480-nm thick Ag<sub>49</sub> Ni<sub>51</sub> and the 510-nm thick Ag<sub>81</sub> Ni<sub>19</sub> thin films on 301 steel are shown in Fig. 2a and 2b, respectively. The contact resistance of the Ag<sub>49</sub> Ni<sub>51</sub>-coated 301 steel remained less than 30 mΩ for 100,000 cycles. The contact resistance of the Ag<sub>81</sub> Ni<sub>19</sub>-coated 301 steel remained 20 mΩ for over 1,000,000 cycles. The fraction of the Ag-rich and Ni-rich phase can thus influence the fretting wear resistance. While the volume fraction of Ni in the Ag<sub>49</sub> Ni<sub>51</sub>, 38%, is above the percolation threshold of 27% <sup>[22]</sup>, the volume fraction Ni in the Ag<sub>81</sub> Ni<sub>19</sub>, 13%, is below this threshold. Above the threshold, the hard phase forms a connected skeleton. Below the threshold, the hard Ni phase disperses into disconnected islands. This experiment shows that a composite coating with islands embedded in a soft Ag matrix has better fretting wear resistance than that of Ag-Ni composite made of a connected Ni skeleton.

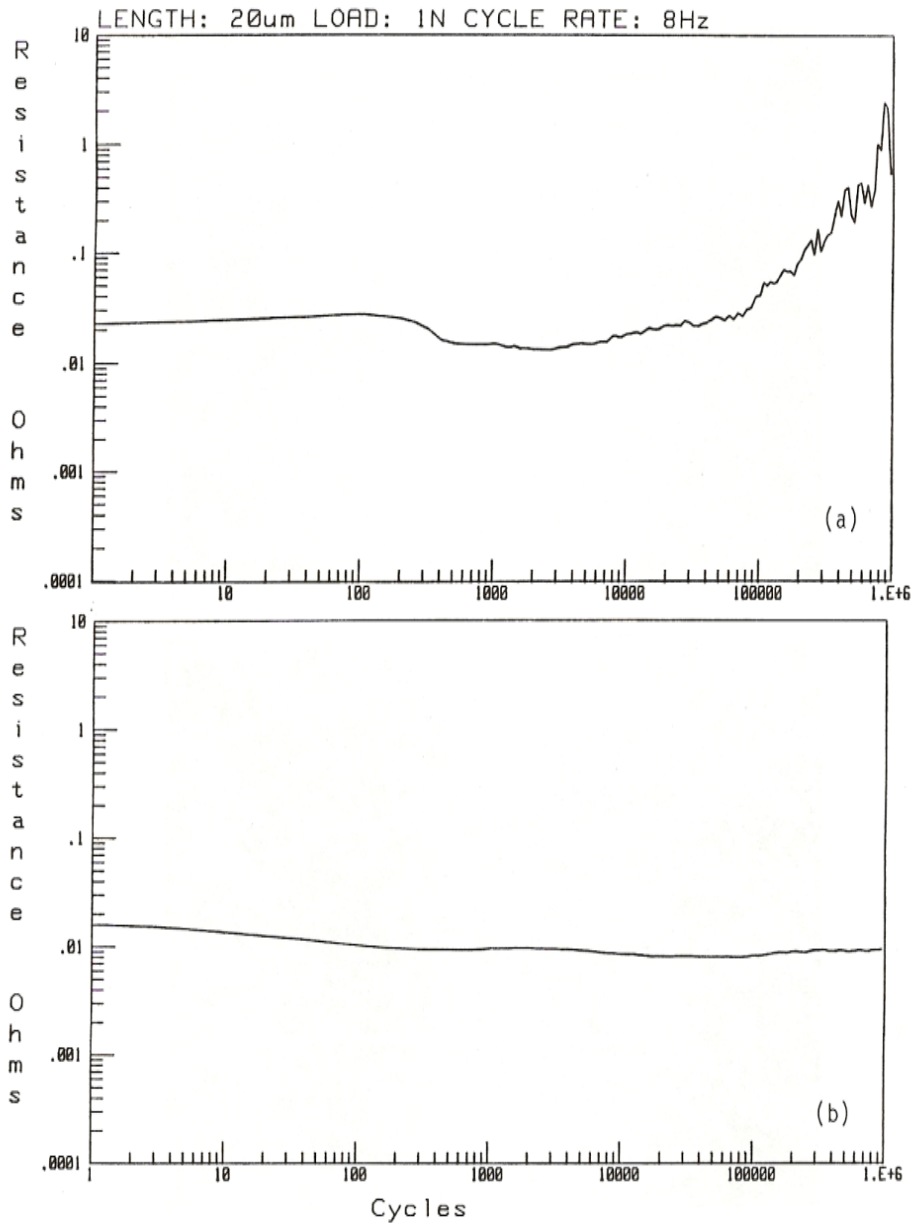


**Figure 2.** Electrical contact resistance versus fretting wear cycles of the Ag<sub>49</sub>Ni<sub>51</sub> nanocrystalline composite film 480-nm thick (a) and the Ag<sub>81</sub>Ni<sub>19</sub> nanocrystalline composite film 510-nm thick (b) on 301 stainless steel dimples and flats.

#### *Thermal Stability*

The contact resistance and coefficient of friction of the Ag-Ni coated 301 steel before and after heat-aging in air at 150<sup>0</sup> C for 168 hours are summarized in Table 2. Before heat-aging, the coefficient of friction for the 480-nm thick Ag<sub>49</sub>Ni<sub>51</sub> and the 510-nm thick Ag<sub>81</sub> Ni<sub>19</sub> are 0.5. This friction coefficient is less than that of bulk sliding on bulk Ag. However, it is slightly larger than that of pure Ag thin films of similar thickness deposited on 301 steel. The contact resistance of the Ag<sub>81</sub>Ni<sub>19</sub> is slightly lower than that of Ag<sub>49</sub>Ni<sub>51</sub>, reflecting perhaps the lower electrical

resistivity of Ag than Ni and the smaller volume fraction of Ni in the Ag<sub>81</sub>Ni<sub>19</sub>. After heat-aging, the contact resistance and friction coefficient for the Ag<sub>49</sub>Ni<sub>51</sub> coated 301 steel increased by a factor of 4.5 and 3, respectively. In contrast, the contact resistance for the Ag<sub>81</sub>Ni<sub>19</sub>-coated 301 steel increases from an average of 5.0 to 7.1 mΩ. The friction coefficient remained the same after heat-aging. The Ag<sub>81</sub>Ni<sub>19</sub>-coated 301 steel has the lowest friction coefficient of 0.5 among all the pure Ag and Ag-Ni composites after the heat-aging process.

**Table 2.** Friction coefficient and contact resistance of thin Ag-Ni composite films 301 stainless steel before and after heat-aging in air at 150<sup>0</sup> C for 168 h.

Samples	Friction Coefficient		Contact Resistance	
	Before aging	After aging	Before aging	After aging
Ag <sub>49</sub> Ni <sub>51</sub>	0.5	1.5	6.0	27.0
Ag <sub>81</sub> Ni <sub>19</sub>	0.5	0.5	5.0	7.1

SEM observations after heat-aging show the formation of particles on the originally smooth Ag<sub>49</sub>Ni<sub>51</sub>-coated 301 steel (Figs. 3a and 3b). AES depth profiling suggests that the particles are Ag-covered Ni-oxides on top of the 301 steel surface (Fig. 4). The significant increase in contact resistance is most likely due to the formation of these oxide particles, which have high electrical resistance. The highly corrugated surface can cause a high friction coefficient<sup>[23]</sup>.

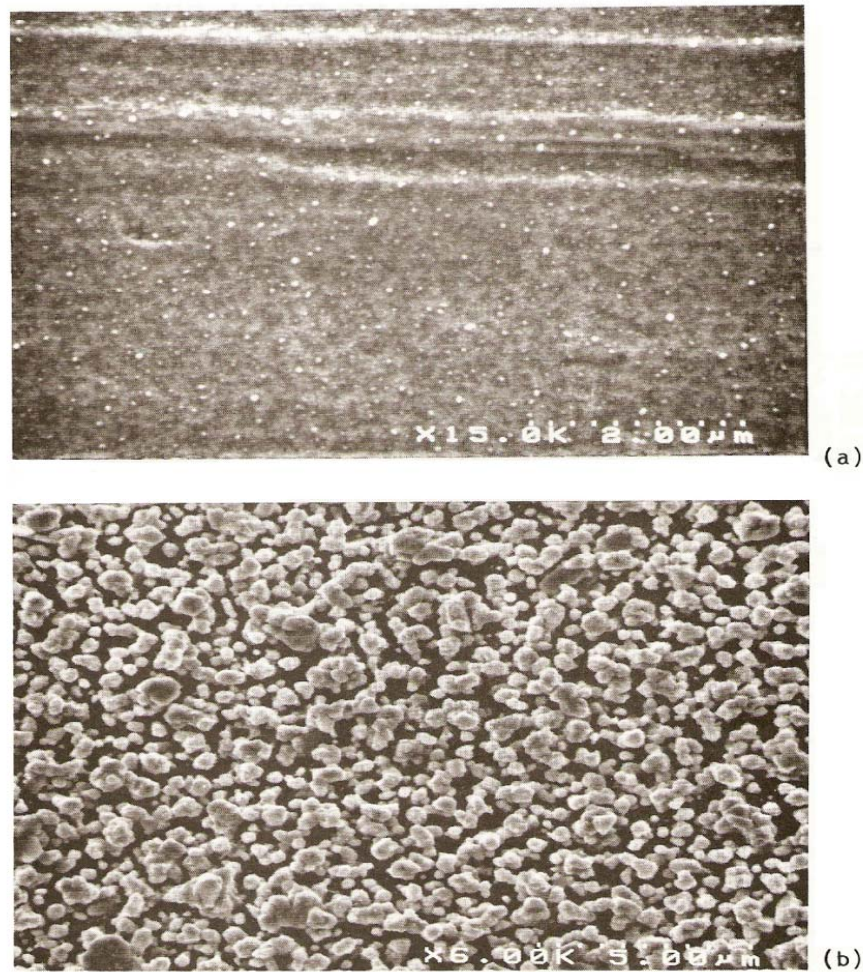


**Figure 3.** Scanning electron microscopy of the Ag<sub>49</sub>Ni<sub>51</sub> nanocrystalline composite films 480-nm thick before (a) and after (b) heat aging in air at 150 °C for 168 hours.

SEM observations after heat-aging show the surface of the originally smooth Ag<sub>81</sub>Ni<sub>19</sub>-coated 301 steel remains smooth with a few large particles (Fig. 5). AES depth profiling suggests that the particles have about the same overall Ag to Ni ratio as the smooth regions. Unlike the Ag<sub>49</sub>Ni<sub>51</sub> coating, oxygen concentration is very low inside the particles and under the surface of the smooth regions of the Ag<sub>81</sub>Ni<sub>19</sub> composite coating. In contrast to the Ag-coated 301 steel, the oxide layer is absent at the interface between the Ag<sub>81</sub> Ni<sub>19</sub> mating and the 301 steel substrate (Fig. 6). Consequently, the contact resistance and friction coefficient change little after heat-aging. Clearly, the resistance to oxidation depends on the appropriate amount of Ni, though similar thickness deposited on 301 steel. The contact resistance of the Ag<sub>81</sub>Ni<sub>19</sub> is slightly lower than that of Ag<sub>49</sub>Ni<sub>51</sub>, reflecting perhaps the lower electrical resistivity of Ag than Ni and the smaller volume fraction of Ni in the Ag<sub>81</sub> Ni<sub>19</sub>.



After heat-aging, the contact resistance and friction coefficient for the Ag<sub>49</sub>Ni<sub>51</sub>-coated 301 steel increase by a factor of 4.5 and 3, respectively. In contrast, the contact resistance for the Ag<sub>81</sub>Ni<sub>19</sub>-coated 301 steel increases from an average of 5.0 to 7.1 mΩ. The friction coefficient remained the same after heat-aging. The Ag<sub>81</sub>Ni<sub>19</sub>-coated 301 steel has the lowest friction coefficient of 0.5 among all the pure Ag and Ag-Ni composites after the heat-aging process. SEM observations after heat-aging show the formation of particles on the originally smooth Ag<sub>49</sub>Ni<sub>51</sub>-coated 301 steel (Figs. 3a and 3b). AES depth profiling suggests that the particles are Ag-covered Ni-oxides on top of the 301 steel surface (Figure 4). The significant increase in contact resistance is most likely due to the formation of these oxide particles, which have high electrical resistance. The highly corrugated surface can cause a high friction coefficient [23].

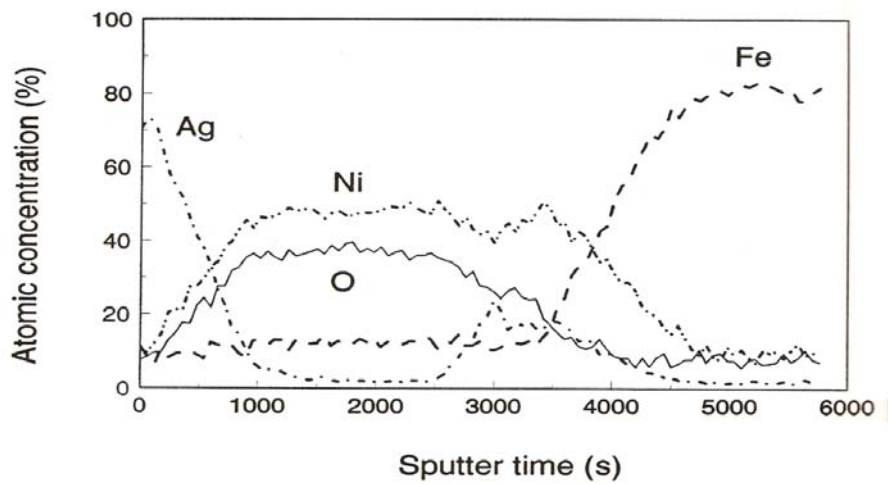


**Figure 4.** The Auger sputtering depth profile of the Ag<sub>49</sub>Ni<sub>51</sub> nanocrystalline composite film 480-nm thick on 301 stainless steel after heat aging in air at 150 °C for 168 hours.

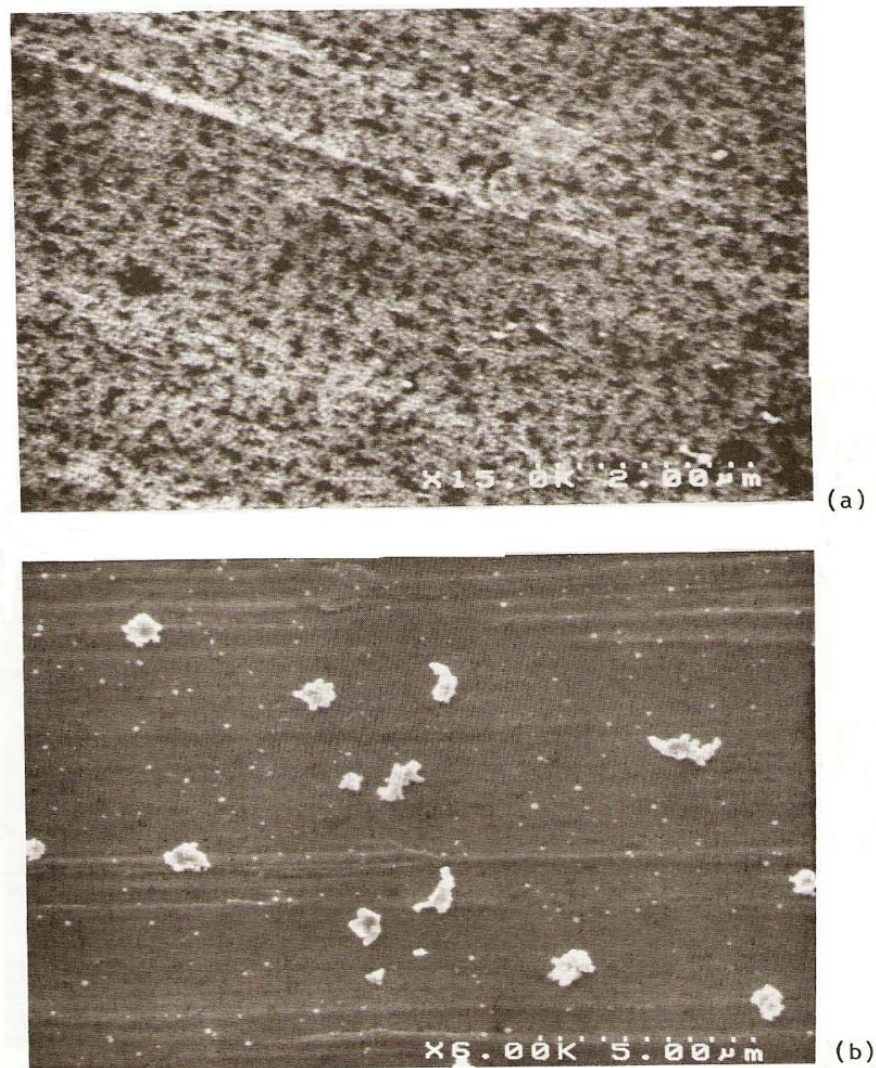


**Figure 5.** Scanning electron microscopy of the  $\text{Ag}_{81}\text{Ni}_{19}$  nanocrystalline composite films 510-nm thick before (a) and after (b) heat aging in air at 150 °C for 168 hours.

SEM observations after heat-aging show the surface of the originally smooth  $\text{Ag}_{81}\text{Ni}_{19}$ -coated 301 steel remains smooth with a few large particles (Fig. 5). AES depth profiling suggests that the particles have about the same overall Ag to Ni ratio as the smooth regions. Unlike the  $\text{Ag}_{49}\text{Ni}_{51}$  coating, oxygen concentration is very low inside the particles and under the surface of the smooth regions of the  $\text{Ag}_{81}\text{Ni}_{19}$  composite coating. In contrast to the Ag-coated 301 steel, the oxide layer is absent at the interface between the  $\text{Ag}_{81}\text{Ni}_{19}$  mating and the 301 steel substrate (Fig. 6). Consequently, the contact resistance and friction coefficient change little after heat-aging. Clearly, the resistance to oxidation depends on the appropriate amount of Ni, though the mechanisms of this oxidation resistance have not been clearly understood. Interdiffusion between both Ag-Ni composite coatings and the 301 steel substrates is absent during heat-aging process (Figs. 4 and 6).

The problem of forming inter- metallics at the Sn/brass interface can thus be avoided by using Ag or Ag-Ni composite coatings on 301 steel.

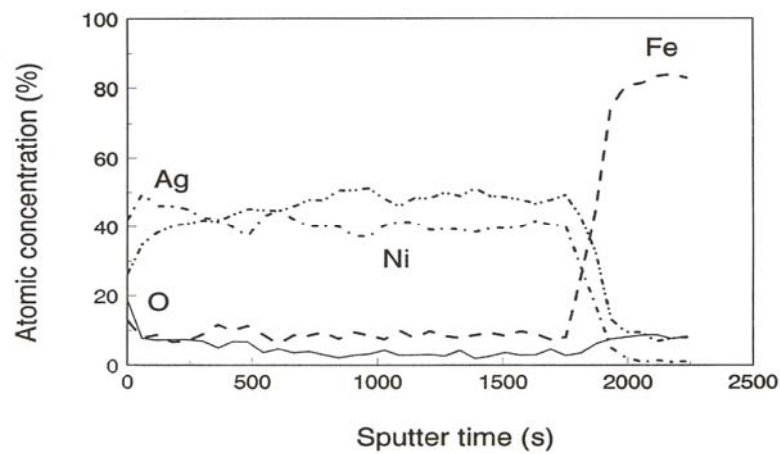


**Figure 6.** The Auger sputtering depth profile of the Ag<sub>81</sub>Ni<sub>19</sub> nanocrystalline composite film 510-nm thick on 301 stainless steel after heat aging in air at 150 °C for 168 hours.

## Conclusion

A metal coating of silver-nickel composite was developed for electrical contact applications with low friction, good wear resistance and low contact resistance. This gives automotive industry competitive advantage in coatings that require good wear resistance and low friction as well as low contact resistance. The results also show that physical vapor deposition can be used to create novel coatings that are either difficult or impossible to make by conventional plating methods.

## References

- [1] Liao, K. C.; Chang, C. C., *Materials and Design*, 2009, 30, 194-199.
- [2] Shigam, N.; Ivery, D.; Chen, W., *J. power sources*, 2008, 183, 651-659.
- [3] Novak, I.; Elyashevick, G. K.; Saprykive, N., *European Polymer Journal*, 2007, 44(8), 2702-2707.
- [4] Kuo, J. K.; Chen, C-K., *J. power sources*, 2006, 162, 207-214.
- [5] Chang, H.; Pitt, C. H.; Alexander, G. B., *Materials Science and Engineering B*, 1991, 8(2), 99-105.
- [6] Tatsuma, T.; Suzuki, K., *Electrochemistry Communications*, 2007, 9, 574-576.
- [7] Drinkaus, P.; Armstrong, T.; Foulka, J., *Applied Ergonomics*, 2008, 5, 72.
- [8] Milus, A.; Greiner, J.; Ries, J. G., *Colloids and Surfaces*, 1992, 63, 281.
- [9] Flynn, A. M.; Brooks, R. A.; Wells III, W. M.; Barell, D. S., *Sensors and Actuators*, 1989, 20, 187.
- [10] Liao, K. C., and Chang, C. C., *Materials and Design*, 2008, 4, 47.
- [11] Zhao, P., and Pecht, M., *Microelectronics Reliability*, 2003, 43, 775.
- [12] Jodeh, S., *Materials Chemistry and Physics*, 2008, submitted.
- [13] Plumb, S., *Ward's Auto World*, August, 34 (1991).
- [14] Nakamura, A., and Takahashi, M., ICEC'92 Proceedings of the Sixteenth International Conference on Electrical Contacts (Loughborough University of Technology, Loughborough, 1992), 97.
- [15] Jodeh, S., *Jordan Journal of Chemistry*, 2008, 3(2), 189-198.
- [16] X-Ray Powder Diffraction File No. 4-850(JCPDS-ICDD), Swarthmore, 1993.
- [17] Haasen, P., *Physical Metallurgy* (Cambridge Univ., Cambridge, 1978), 133.

- [18] de Boer, F. R.; Boom, R.; Mattens, W. C. E., Cohesion in Metals, North Holland, Amsterdam, 1989.
- [19] Singleton, M.; Nash, P., in Binary Alloy Phase Diagrams Vol. 1, Second Edition, edit.ed by T. B. Massalski (ASTM International, Materials Park, 1990), 64.
- [20] Adams, D.; Atzmon, M.; Srolovitz, D., *J. Mater. Res.*, 1992, 7, 653-658.
- [21] Tung, S., United States Patent, 5,225,253 (1993).
- [22] Zallell, R., The Physics of Amorphous Solids John Wiley & Sons, New York, 1983, 186.
- [23] Rabinowicz, E., Friction and Wear of Materials John Wiley & Sons, New York, 1965, 66.